DOI 10.24425/pjvs.2025.154010

Original article

Research on expression patterns of endogenous OASL and IFN-α in duck embryos infected with DHAV-3

H. Zhang[#3], Y. Tang[#1,2] , X. Hong[1,2], S. Zhou[1,2] , T. Zhang[1,2]

[1] Institute of Comparative Medicine, College of Veterinary Medicine, Yangzhou University, Yangzhou, Jiangsu 225009, China
[2] Jiangsu Co-innovation Center for Prevention and Control of Important Animal Infectious Diseases and Zoonoses, Yangzhou, Jiangsu 225009, China
[3] Independent researcher, New York, NY 11355, USA

Correspondence to: T. Zhang, e-mail: slx@yzu.edu.cn
# These authors contributed equally to this work and should be considered co-first authors

Abstract

An animal body's immune response to viruses might vary depending on various factors. The relationship between 2'-5'-oligoadenylate synthetase like (OASL), interferon alpha (IFN-α), and duck hepatitis A virus type 3 (DHAV-3) virus genome copy number in duck embryo tissues was studied to investigate duck's natural antiviral immunity mechanism. 15-day-old SPF duck embryos were infected with DHAV-3 and their organs and tissues were collected at various times after inoculation. RT real-time PCR was used to determine *OASL* and *IFNA* mRNA expression levels and the DHAV-3 copy number. Compared with that at 0 hours, liver *OASL* transcription increased significantly at 24 hours, and extremely significantly in the liver, heart, gizzard, small intestine, and muscle at 48 hours. The heart had the highest expression level, followed by the liver, with lower expression in the other tissues. There was no significant difference in *IFNA* expression between the heart and liver at 12 hours, but it started to rise at 24 hours, reaching its maximum at 48 hours. Although *IFNA* expression increased in the gizzards, small intestines, and muscles, its relative expression levels were lower than those in the heart and liver. In the tissues, the virus genome copy number peaked at 24 hours, and then decreased. The liver had the highest virus genome copy number, followed by the heart. The results implied that the differences in *OASL* transcription in the tested tissues were similar to those of IFNA. Thus, the immune response (OASL and IFN-α levels) of duck embryos to DHAV-3 shows tissue differences, especially in the liver and heart.

Keywords: duck, immunity, tissue specificity, viral infection

Introduction

Duck virus hepatitis (DVH) is an infectious disease caused by duck hepatitis virus (DHV), characterized by hemorrhagic liver disease and often accompanied by neurological symptoms. Duck hepatitis A virus (DHAV) is one of the pathogens that cause fatal DHV in ducklings, which is an acute and contagious disease with a high mortality rate that seriously jeopardizes the duck industry worldwide (Yugo et al. 2016). DHAV is a member of the genus *Avihepatovirus*, family *Picornaviridae* and is the only species in this genus (ICTV). Historically, DVH was subdivided into types I, II, and III (Levine and Fabricant 1950, Tseng and Tsai 2007, Wang et al. 2008, Kim et al. 2009). The routine vaccination of domestic breeding ducks and ducklings against DHAV-1 probably results in a reduced risk for virus spread; however, the existing DHAV-1 vaccine cannot provide protection against DHAV-3, resulting in widespread prevalence of DHAV-3 in mainland China, where it represents an important pathogen causing substantial losses to the Chinese duck industry (Wen et al. 2018, Fehér et al. 2021, Zhang et al. 2023, Ye et al. 2023).

The innate immune response of the host provides the first line of defense against viral infection. In the cellular response to pathogen invasion, the host recognizes some conserved non-self molecules, termed pathogen-related molecular patterns (PAMP), such as retinoic acid-induced gene I (Rig-I), and activates downstream antiviral factors (including Interferon alpha (IFN-α), Interferon-β (IFN-β), Protein Kinase R (PKR), 2'-5' Oligoadenylate Synthetase (OAS)) and upregulates inflammatory cytokines (including interleukin (IL)-6, TNF-α, IL-1β, IFN-γ, IFN-γ) (Xie et al. 2018) to combat viruses, including antiviral defense, anti-proliferative activity, and stimulation of adaptive immunity (Schneider et al. 2014). Currently, there is an emerging understanding of the role of cytokine in tissue homeostatic functional regulation and it is becoming clear that pathological conditions may develop from dysregulation of cytokines (Tjiong et al. 1999, Kutlu et al. 2003, Peinnequin et al. 2003). For example, the molecular interactions within the IL-6/IL-12 cytokine/receptor superfamily, highlighting the structural features that govern receptor specificity and signaling efficiency, critical for the immune response (Jones et al. 2011). 2'-5'-oligoadenylate synthetase like (OASL) has broad-spectrum antiviral activity, and is induced by type I interferon and expressed in almost all vertebrates. OAS has 2'-5' oligoadenylate synthetase activity, allowing it to degrade RNA in infected cells through the classical OAS/RNaseL pathway, thereby effectively preventing the replication of RNA viruses. OASL lacks the oligoadenylate synthetase activity, and mainly exerts its antiviral effect through the OASL/RIG-I pathway, degrading RNA in infected cells (Ishibashi et al. 2010, Zhu et al. 2014, Yang et al. 2017). Despite being one of the natural immune proteins, OASL is rarely reported in the data of virus replication and immune responses of different tissues of ducks. An animal's bodily immune response might vary depending on factors such as animal age, tissue, and the variety and virulence differences of virus strains. In the present study, the relative mRNA expression of *OASL* and *IFNA*, and the DHAV-3 genome copy number were measured, and a method of amplifying DHAV-3 by infecting duck embryos was developed. The objectives were as follows: 1. To study endogenous OASL and IFN-α expression patterns in different tissues of duck embryos; 2. To study the different immune responses of different tissues of duck embryos to DHAV-3; 3. To investigate the relationship between OASL, IFN-α and viral load in duck embryo tissues and organs, and to explore OASL, IFN-α transcription trends and DHAV-3 proliferation. This study presents a good animal model to study the replication of RNA viruses in human tissues and the immune response of the body (Ishibashi et al. 2010).

Materials and Methods

Experimental animals and strains

The DHAV-3 strain (112803) was a gift from Zhang Dabing of the Beijing Agricultural University. Specific pathogen free (SPF) duck embryos were purchased from Shandong Hao Tai Experimental Animal Breeding Company Limited (Jinan, China). Specific pathogen-free (SPF) embryos are distinct from gnotobiotic embryos, which are completely germ free and require sterile facilities. Ethics approval and consent to participate were not required for this type of study.

DHAV-3 virus proliferation and ELD_{50} (50% lethal dose for embryos) determination

Five per group 9 day old SPF duck embryos were randomly divided into an experimental group and a control group. The experimental group was inoculated with 0.2 mL of DHAV-3 virus solution into the allantoic cavity, and the virus was continuously passed through three passages, recovered, and stored in a –70°C freezer.

The virus solution was diluted 10-fold with saline and injected into the allantoic cavity of 9-day-old duck embryos (at 10^{-2}, 10^{-3}, 10^{-4}, 10^{-5} and 10^{-6} dilutions). The virus genome copy number per μL of inoculum was used to evaluate as virus titration value. Each embryo

Table 1 . DHAV-3 gene Primers.

Target gene	Fragment length	Primer sequences (5'-3')	GenBank accession No.
β-actin	199bp	CCCCATTGAACACGGTATTGTC	AJ312193.1
		GGCTACATACATGGCTGGGG	
OASL	187bp	TCTTCCTCAGCTGCTTCTCC	KY775584.1
		ACTTCGATGGACTCGCTGTT	
DHAV-3	145bp	CTTGAACGTAATAGAGCTTGG	KM267028.1
		AGTCTTTTGGTAGAGTCTTAG	
IFN-α	232bp	TCCTCCAACACCTCTTCGAC	HQ680866.1
		GGGCTGTAGGTGTGGTTCTG	

was injected with 0.2 mL. Each concentration of virus was injected into five duck embryos, and the number of dead duck embryos within 7 days was counted. The ELD_{50} was then calculated using the Reed Munch method (Reed et al. 1938).

DHAV-3 Genome copy number Standard Curve

According to the DHAV-3 gene sequence in the NCBI database, primers were designed using Primer 5.0 (Table 1) and synthesized by Yingwei Jieji (Shanghai) Trading Co., Ltd. The viral RNA of DHAV-3 was extracted from duck embryo allantoic fluid using an RNA extraction kit (TIANGEN) and subjected to reverse transcription PCR (RT PCR) which was performed using a PrimeScript™ RT Reagent Kit (Perfect Real Time, TaKaRa). The DHAV-3 PCR product was recovered and ligated into vector pMD19T. The constructed pMD19TDHAV-3 plasmid was extracted from the cells and diluted 10-fold. The plasmid at different concentrations was used as a template to establish standard curves and melting curves. Real-time fluorescence quantitative analysis was carried out using an SYBR Green Super-Real Fluorescence Quantitative Premixed Reagent (TIANGEN) and a Step One™ Real-Time PCR System (Applied Biosystems).

DHAV-3 inoculation on *OASL* mRNA expression and the viral load

According to the *ACTB* (encoding β-actin), *OASL*, DHAV-3, and *IFNA* gene sequences in the NCBI gene database, primers were designed using Primer 5.0 and synthesized (Table 1).

Fifteen-day old SPF duck embryos were inoculated with DHAV-3 at 10^3 ELD_{50} through the allantoic cavity, with five duck embryos being inoculated at each time point. The hearts, liver, gizzards, small intestines, and thigh muscles were sampled at 6, 12, 24, and 48 h after inoculation and stored in liquid nitrogen. Five untreated SPF duck embryos comprised the 0 h blank control. Total RNA was extracted from the tissues and reverse transcribed to synthesize cDNA, which was used as the template for quantitative real-time PCR (qPCR or fluorescence quantitative PCR).

The experimental results of fluorescence quantitative PCR were analyzed using the $2^{\Delta\Delta CT}$ method, and the genome copy number of the virus was determined by the expression level of DHAV-3 according to the Cq (cycle of quantity) value of the standard curve. A T test was used for the statistical analysis of the differences between the two groups, with GraphPad Prism 8.0 (GraphPad Inc., La Jolla, CA, USA) being used for the statistical analysis.

Results

DHAV-3 virus proliferation and ELD_{50}

After duck embryo passage, there was no bacterial infection in the virus solution. After passage, the time to duck embryo death was shortened. According to the Reed-Muench method, the ELD_{50} of DHAV-3 (112803) toward 9-day-old duck embryos was $10^{-4.5}$/0.2 mL. The viral titer is the number of genome copies per microliter of inoculum.

DHAV-3 Genome copy number Standard Curve

The extracted viral RNA was reverse transcribed using specific primers and subjected to electrophoresis detection. The length of the amplified fragment was approximately 150 bp, which was consistent with the target fragment length. The target fragment of DHAV-3 was ligated into pMD-19T and transformed into *E. coli*. Amplification and plasmid extraction were carried out, and the plasmid pMD19T-DHAV-3 was digested and identified. The positive bacterial clone was sent to Anhui Huaheng Biotechnology Co. Ltd. (Hefei, China) for Sanger sequencing. The results were compared with the sequence deposited at the NCBI using BLAST and confirmed as a DHAV-3 band, showing a nucleotide identity of 98% with the reference

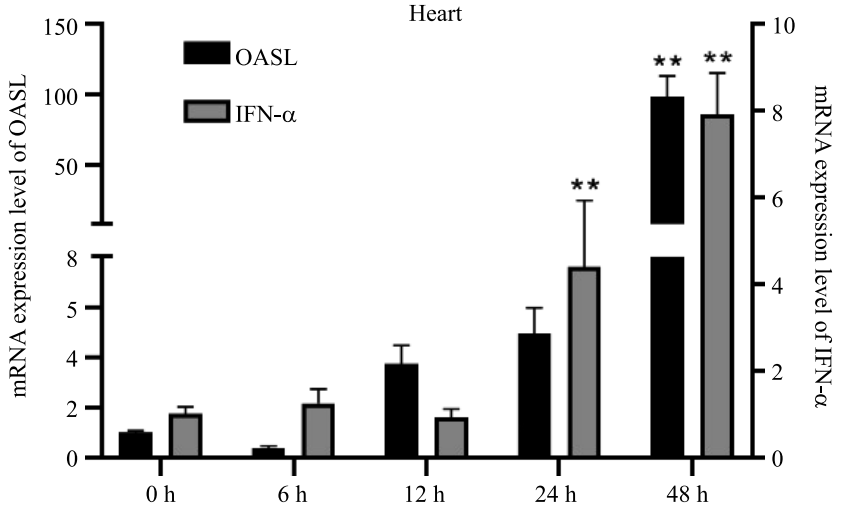

Fig. 1. qPCR to detect relative mRNA of heart in duck embryonated eggs.

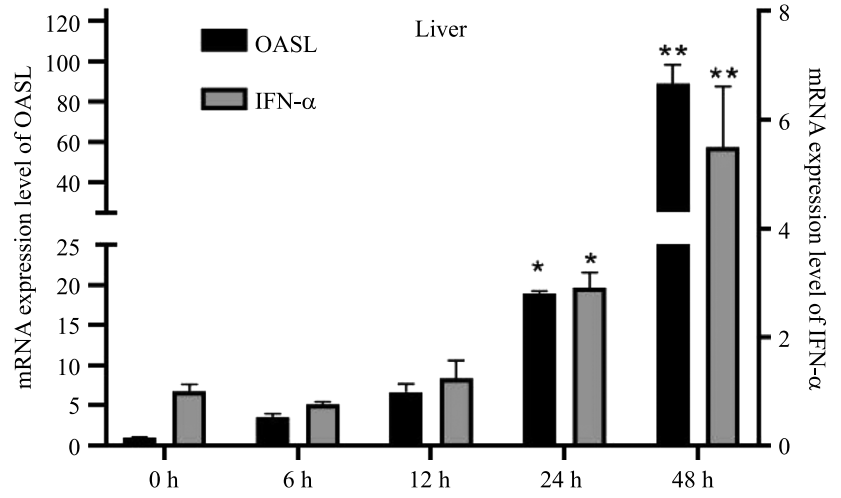

Fig. 2. qPCR to detect relative mRNA of liver in duck embryonated eggs.

sequences. The genome copy number concentration of the pMD19T-DHAV-3 plasmid was 6.8×10^{10} copies/μL. The concentration was then diluted to eight gradients of 6.8×10^{8} to 6.8×10^{1}, each of which was added to a 20 μL reaction system for qPCR. The results of qPCR were used to produce a dissolution curve and a standard curve. The standard curve is represented by y = -3.221x+30.593, and the correlation coefficient R^2 = 0.9977. The amplification efficiency E value of qPCR was 2.04.

Expression of *OASL* and *IFNA* mRNA and the viral load at different times after DHAV3 infection of SPF duck embryos

OASL and *IFNA* mRNA expression in the heart of SPF duck embryos inoculated by DHAV-3

After the duck embryos were inoculated by 10^3 ELD50 DHAV-3 for 0, 6, 12, 24, and 48 h, qPCR was used to detect the relative contents of *OASL* and *IFNA* mRNA in the heart (Fig. 1). Compared with that at 0 h, *OASL* expression decreased at 6 h, began to increase at 12 h, and reached a maximum at 48 h ($p<0.01$). *IFNA* expression did not change significantly within 12 h, but began to increase at 24 h, reaching a maximum at 48 h ($p<0.01$).

OASL and *IFNA* mRNA expression in the liver of SPF duck embryos inoculated by DHAV-3

After inoculating duck embryos with 10^3ELD_{50} DHAV-3 for 0, 6, 12, 24, and 48 h, qPCR was used to detect *OASL* and *IFNA* mRNA expression in the liver (Fig. 2). Compared with that at 0 h, *OASL* expression continued to increase within 24 h, was significantly increased at 24 h, and reached its maximum at 48 h ($p<0.01$). Compared with that at 0 h, the *IFNA* expression level did not significantly change within 12 h, but was significantly upregulated at 24 h and reached its maximum at 48 h ($p<0.01$).

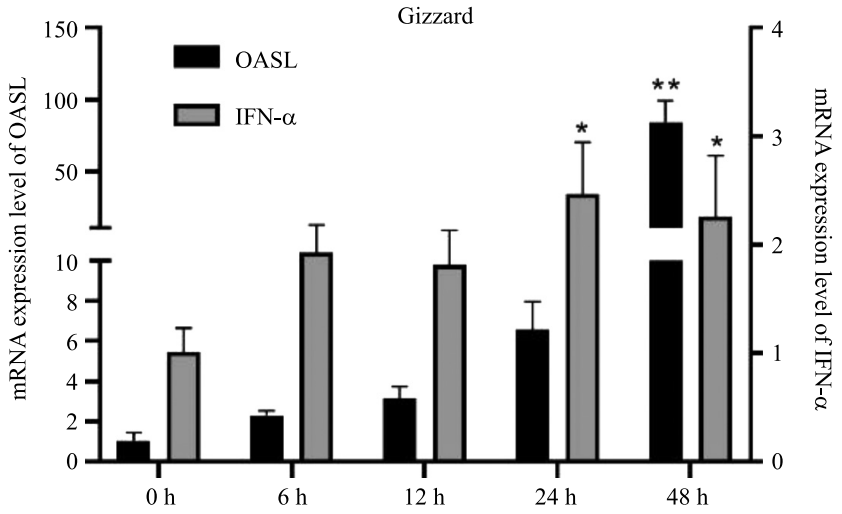

Fig. 3. qPCR to detect relative mRNA of gizzard in duck embryonated eggs.

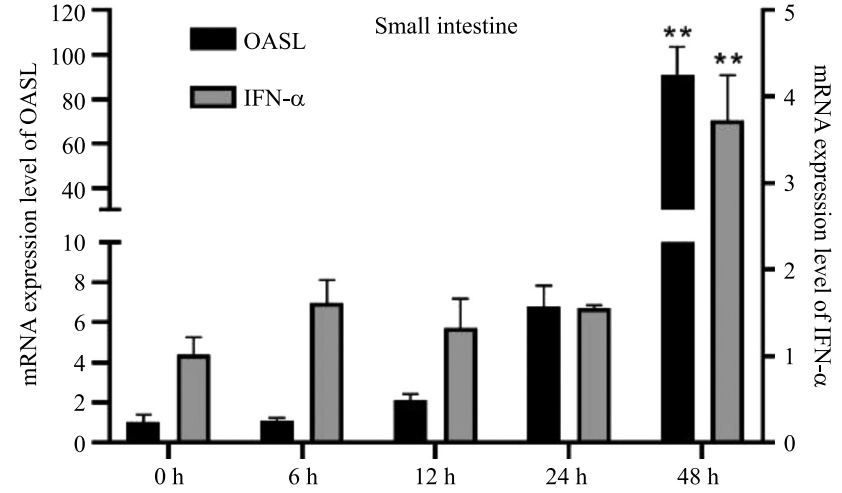

Fig. 4. qPCR to detect relative mRNA of small intestine in duck embryonated eggs.

OASL and *IFNA* expression in the gizzard of SPF duck embryos inoculated by DHAV3

After inducing duck embryos with 10^3 ELD_{50} DHAV-3 for 0, 6, 12, 24, and 48 h, qPCR was used to detect *OASL* and *IFNA* mRNA expression in the gizzard (Fig. 3). Compared with that at 0 h, *OASL* expression continued to increase within 24 h and reached its maximum value at 48 h ($p<0.01$). Compared with that at 0 h, *IFNA* expression began to increase within 12 h, and remained stable at 24 and 48 h ($p<0.01$).

OASL and *IFNA* expression in the small intestines of SPF duck embryos inoculated by DHAV-3

After inducing duck embryos with 10^3 ELD_{50} DHAV-3 for 0, 6, 12, 24, and 48 h, qPCR was used to detect *OASL* and *IFNA* mRNA expression in the small intestines (Fig. 4). Compared with that at 0 h, *OASL* expression continued to increase within 24 h and reached its maximum value at 48 h ($p<0.01$). Compared with that at 0 h, *IFNA* expression did not change significantly within 24 h, but increased very significantly at 48 h ($p<0.01$).

OASL and *IFNA* expression in the thigh muscle of SPF duck embryos inoculated by DHAV-3

After inducing duck embryos with 10^3 ELD_{50} DHAV-3 for 0, 6, 12, 24, and 48 h, qPCR was used to detect *OASL* and *IFNA* mRNA expression in the thigh muscle (Fig. 5). Compared with that at 0 h, *OASL* expression was continuously upregulated up to 48 h, being significantly expressed at 24 h ($p<0.05$), and extremely significantly expressed at 48h ($p<0.01$); Compared with that at 0 h, the *IFNA* expression level did not change significantly within 12 hours, but increased very significantly after 24 h ($p<0.01$).

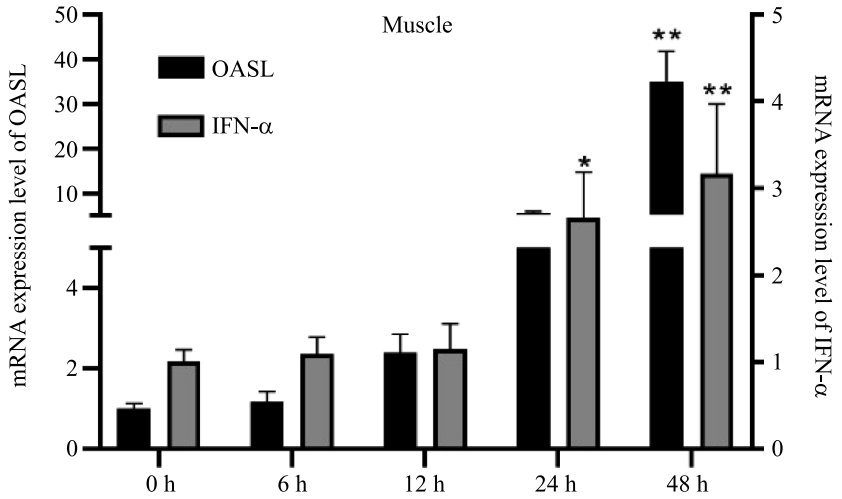

Fig. 5. qPCR to detect relative mRNA of muscle in duck embryonated eggs.

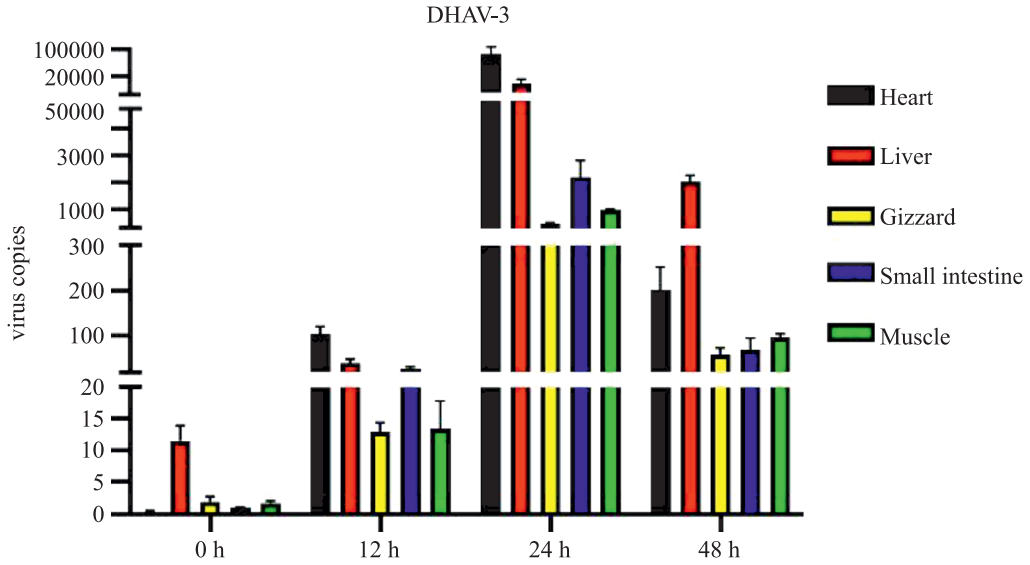

Fig. 6. qPCR to detect virus genome copies in each tissue of duck embryonated eggs.

Virus genome copy numbers in sampled tissues of duck embryos inoculated by DHAV-3

After inducing duck embryos with 10^3 ELD_{50} DHAV-3 for 0, 6, 12, 24, and 48 h, qPCR was used to detect DHAV-3 levels in tissue. The results showed that the virus replication was detected in the liver at 6 h, and the virus was almost undetectable in the other tissues. By 12 h, replication was detected in the hearts, gizzards, small intestines, and muscles. The virus genome copy number reached its peak between 24 and 48 hours, and the maximum virus genome copy number was reached in the liver at 48 h, followed by the heart and other tissues (Fig. 6).

Discussion

DHAV can be amplified in ducks, duck embryos, chicken embryos, and avian cells (Woolcock et al. 1982, Luo et al. 1996, Su et al. 2002, Fu et al. 2012). Using SPF duck embryos as experimental materials, the influence of other pathogenic bacteria and variable maternal antibodies can be excluded. A model comprising experimental duck hepatitis B virus (DHBV) infection as the infective supernatant is also more suitable for the DHBV virus biological research because of its stability and practicability. A standard DHBV model was therefore established, which is conducive to studying the interaction between the virus and OASL and IFN-α. It is also beneficial to study duck's antiviral strategies. The earliest outbreak of duck viral hepatitis in mainland China was caused by DHAV-1. However, as mentioned earlier, a recent epidemiological survey reported that DHAV-3 has become the pre-

dominant serotype in Asian areas. Therefore, this study selected a DHAV-3 virus strain.

In this study, compared with that at 0 h, DHAV-3 induced a significant increase in *OASL* transcription in the liver of SPF duck embryos at 24 h, and a very significant increase in *OASL* transcription in the liver, heart, gizzard, small intestine, and muscle at 48 h. The highest expression level was reached in the heart, followed by the liver, and the relative expression in the gizzard, small intestine, and muscle was much lower than that in the liver and heart. There was no significant difference in *IFNA* expression between the heart and liver in the first 12 hours, but it began to increase at 24 h and reached the maximum at 48 hours. The expression in the gizzard, small intestine and muscle increased slowly; however, the relative expression of *IFNA* was lower than that in the heart and liver.

The OAS family genes in poultry are different from those in mammals, with only the OASL gene being found (Bi et al. 2017)**.** DHAV infection in ducks immediately activates the body's innate immune system and activates a large number of pattern recognition receptors and downstream antiviral factors (e.g. OASL and IFN-α) to degrade RNA in infected cells to fight against the virus (Perelygin et al.2006, Zhu et al. 2014). The activation and expression of interferon genes represent the first line of defense for hosts against virus invasion, and DHAV-3 induces high levels of IFNA gene expression in the liver, which would help to establish the body's innate immune system.

DHAV-3 shows extensive tissue tropism in ducklings. The liver, spleen, and kidney are the main target organs of DHAV-3 attack, and cytokines in the liver play an important role in inhibiting virus proliferation and repairing tissue damage, and *IFNA* showed the highest transcription in the liver and kidney (Zhu et al. 2018, Ou 2021).

Our analysis indicated that *IFNA* transcription in the heart was second only to that in the liver in duck embryos after DHAV-3 induction. The difference in transcription level of *OASL* in different tissues was similar to that of IFNA. In this study, infection of duck embryos with DHAV-3 112803 caused extensive bleeding. Virus replication was detected in the liver at 6 h after DHAV-3 inoculation, and the virus reached the maximum genome copy number in the liver at 48 h, followed by the heart. DHAV-3 inoculation induced the highest IFNA transcription in the liver, which also suggests that the liver is the most important target organ for DHAV infection and replication. When the abundance of the virus in the main target organs reaches a certain level, the virus will "overflow" to other organs, such as the heart, spleen, kidneys, and gastrointestinal tract.

The pathogenic mechanism of DHAV is mainly that the virus invades the body of ducklings and causes the greatest damage to the liver. DHAV can replicate at a high level in the liver tissue of ducklings and persists, leading to bleeding, deformation, and necrosis of the liver tissue (Zhang et al. 2012, Ou et al. 2017, Cao et al. 2020). However, the existence of significant viral antigens in the heart varies. In 2007, Zhu dynamically observed the virus distribution in ducklings artificially infected with DHAV. The results showed that DHAV could be detected in the liver, spleen, and pancreas, while virus antigens were not detected in the kidneys and heart (Zhu et al. 2007). In 2018, ducklings were infected with a strong DHAV-3 virus, and 11 tissue samples of ducklings were tested for virus content and antiviral cytokines (IFN) in the liver. DHAV-3 was found to have a wide range of tissue preferences in the ducklings, with the liver and spleen being the main target organs, although the heart was not mentioned in the study (Zhu et al. 2018). In contrast to the above research, in 1996, Cheng observed tissue sections of artificially infected ducklings with DHV at 3 h after infection, and virus antigens were present in the cytoplasm of the hearts, liver, spleen, kidneys, and leg muscles of the ducklings (Cheng et al. 1996). In 1997, Wang detected the virus distribution in 1-day-old ducklings artificially infected with DHV. The results showed that the order of DHV high virulence was the heart, kidney, lung and chest muscle, but not in liver and small intestine. When attenuated DHV was injected, the order of DHV levels in ducklings' tissues was heart, liver, spleen, lung, and kidney (Wang et al. 1997). Wei inoculated ducklings with DHAV-3, and the virus could be detected in the heart, liver, small intestine and other tissues at 1 h after induction using real-time fluorescence quantitative PCR, and the genome copy number of the virus was significantly increased within 24 hours (Wei 2020). In this study, we clearly demonstrated that for duck embryos, the heart is a target organ for DHAV-3 attack.

The time of virus detection in different tissues varied, which may be related to the difference in the immune mechanism of animals at different growth stages. Song reported that the expression levels of innate immune related factors in 3-week-old ducklings inoculated by DHAV were significantly higher than those in 1-day-old ducklings (Song et al. 2014).

Conclusion

In this study, the relationship between OASL and IFN-α and tissue virus genome copy number in some tissues of duck embryos infected with DHAV was

examined. The immune responses (as assessed using OASL and IFN-α levels) of duck embryo tissues to DHAV-3 are different, among which the liver had the highest response, followed by the heart. This indicated that in addition to the liver, the heart is a major target organ of DHAV-3 attack. The study provided a theoretical basis and experimental data for the study of duck's natural immune antiviral mechanism.

Acknowledgements

This project was supported by the 111 Project D18007 and a project funded by the Priority Academic Program Development of Jiangsu Higher Education Institutions (PAPD).

References

Bi K, Han K, Liu Q, Zhao D, Huang X, Liu Y, Yang J, Li Y **(2017)** Molecular cloning, characterization, and expression of duck 2'-5'-oligoadenylate synthetase-like gene. Gene 629: 43-51.

Cao J, Zhang Y, Chen Y, Liang S, Liu D, Fan W, Xu Y, Liu H, Zhou Z, Liu X, Hou S **(2020)** Dynamic Transcriptome Reveals the Mechanism of Liver Injury Caused by DHAV-3 Infection in Pekin Duck. Front Immunol 11: 568565.

Chen, Y, Hu, S, Lin, X, Tian, J, Lv, J, Wang, M, Luo, X, Pei, Y, Hu, R, Song, Z, Holmes, E, Zhang, Y **(2023)**. Host traits shape virome composition and virus transmission in wild small mammals. Cell 186: 4662-4675.e4612.

Cheng G, Hu X, Zhou S, Xiong D**(1996)** Determining the Location of Duck Hepatitis Virus in Inoculated Ducklings by Monoclonal Antibody-pap Technique. J Huazhong Agric Univ. 15: 568-572.

Fehér E, Jakab S, Bali K, Kaszab E, Nagy B, Ihász K, Bálint Á, Palya V, Bányai K**(2021)** Genomic Epidemiology and Evolution of Duck Hepatitis A Virus. Viruses 13: 1352.

Fu Y, Chen Z, Li C, Liu G **(2012)** Establishment of a duck cell line susceptible to duck hepatitis virus type 1. J Virol Methods 184: 41-45.

Ishibashi M, Wakita T, Esumi M**(2010)** 2',5'-Oligoadenylate synthetase-like gene highly induced by hepatitis C virus infection in human liver is inhibitory to viral replication in vitro. Biochem Biophys Res Commun. 392: 397-402.

Jones LL, Vignali DAA **(2011)** Molecular interactions within the IL-6/IL-12 cytokine/receptor superfamily. Immunol Res 51: 5-14.

Kim MC, Kim MJ. Kwon Y K, Lindberg A M, Joh S K, Kwon H M, Lee Y J, Kwon J H **(2009)** Development of duck hepatitis A virus type 3 vaccine and its use to protect ducklings against infections. Vaccine 27: 6688-6694

Kutlu B, Cardozo AK, Darville MI, Kruhøffer M, Magnusson N, Ørntoft T, Eizirik DL **(2003)** Discovery of gene networks regulating cytokine-induced dysfunction and apoptosis in insulin-producing INS-1 cells. Diabetes 52: 2701-2719.

Levine P, Fabricant J **(1950)** A hitherto-undescribed virus disease of ducks in North America. Cornell Vet 40: 71-86.

Luo HL, Fan WM, Zhang JY, Liu JP (**1996**) Research of cell culture technique of duck Hepatitis virus. Jiangsu Agric Sci 06: 53-54.

Ou XM **(2021)** The attenuation of DHAV vaccine and its immune responses in breeding ducks. Master's Thesis. Sichuan Agric Univ. Chengdu, China

Ou X, Mao S, Cao J, Ma Y, Ma G, Cheng A, Wang M, Zhu D, Chen S, Jia R, Liu M, Sun K, Yang Q, Wu Y, Chen X **(2017)** The neglected avian hepatotropic virus induces acute and chronic hepatitis in ducks: an alternative model for hepatology. Oncotarget 8: 81838-81851.

Peinnequin A, Mouret C, Birot O, Alonso A, Mathieu J, Clarençon D, Agay D, Chancerelle Y, Multon E **(2003)** Rat pro-inflammatory cytokine and cytokine related mRNA quantification by real-time polymerase chain reaction using SYBR green. BMC Immunol. 5: 3.

Perelygin AA, Zharkikh AA, Scherbik SV, Brinton MA **(2006)** The mammalian 2'-5' oligoadenylate synthetase gene family: evidence for concerted evolution of paralogous Oas1 genes in Rodentia and Artiodactyla. J Mol Evol 63: 562-576.

Reed LJ, Muench H **(1938)** A simple method of estimating fifty percent endpoints. Am J Epidemiol 27: 493-497.

Schneider WM, Chevillotte MD, Rice CM **(2014)** Interferon--stimulated genes: a complex web of host defenses. Annu Rev Immunol 32: 513-545.

Song C, Yu S, Duan Y, Hu Y, Qiu X, Tan L, Sun Y, Wang M, Cheng A, Ding C **(2014)** Effect of age on the pathogenesis of DHV-1 in Pekin ducks and on the innate immune responses of ducks to infection. Arch Virol 159: 905-914.

Su J, Huang Y, He R, Zhao J, Gu Y **(2002)** Screening and primary identification of new type duck hepatitis virus. Chin J Vet Sci Technol 32: 15-16.

Tjiong MY, van der Vange N, ten Kate FJ, Tjong-A-Hung SP, ter Schegget J, Burger MP, Out TA **(1999)** Increased IL-6 and IL-8 levels in cervicovaginal secretions of patients with cervical cancer. Gynecol Oncol 73: 285-291.

Tseng CH, Tsai HJ **(2007)** Molecular characterization of a new serotype of duck hepatitis virus. Virus Res 126: 19-31.

Wang L, Pan M, Fu Y, Zhang D**(2008)** Classification of duck hepatitis virus into three genotypes based on molecular evolutionary analysis. Virus Genes 37: 52-59.

Wang MS, An AC, Chen XY**(1997)** Study on duck viral hepatitis distribution and excretion of virulent duck H\hepatitis virus in duckling and adult duck Chin J Vet Sci 17: 254-257.

Wei R (2020) Cloning and polymorphism analysis of OASL gene in Gaoyou duck and study on the effect of DHAV-3 on OASL expression. Master's Thesis. Yangzhou Univ. Yangzhou, China

Wen X, Zhu D, Cheng A, Wang M, Chen S, Jia R, Liu M, Sun K, Zhao X, Yang Q, Wu Y, Chen X **(2018)** Molecular epidemiology of duck hepatitis a virus types 1 and 3 in China, 2010–2015. Transbound Emerg Dis 65: 10-15.

Woolcock PR, Chalmers WS, Davis D **(1982)** A plaque assay for duck hepatitis virus. Avian Pathol 11: 607-610.

Xie J, Wang M, Cheng A, Zhao X, Liu M, Zhu D, Chen S, Jia R, Yang Q, Wu Y, Zhang S, Liu Y, Yu Y, Zhang L, Sun K, Chen X **(2018)** Cytokine storms are primarily responsible for the rapid death of ducklings infected with duck hepatitis A virus type 1. Sci Rep 8: 6596.

Yang C, Chen S, Wang MS, Cheng AC **(2017)** Research progress of the association between the 2', 5'-oligoadenylate synthetase and antiviral mechanism. Chin J Prev Vet Med 39: 682-685.

Ye L, Zhou S, Zhang H, Zhang T, Yang D, Hong X **(2023)** A meta-analysis for vaccine protection rate of duck hepatitis a virus in mainland China in 2009-2021. BMC Vet Res 19: 179.

Yugo DM, Hauck R, Shivaprasad HL, Meng XJ **(2016)** Hepatitis virus infections in poultry. Avian Dis 60: 576- 588.

Zhang H, Pi J, Tang C, Yue H, Yang F**(2012)** An experimental study of the pathogenicity of a duck hepatitis A virus genotype C isolate in specific pathogen free ducklings. Avian Pathol 41: 613–620.

Zhang Y, Wu S, Liu W, Hu Z**(2023)** Current status and future direction of duck hepatitis A virus vaccines. Avian Pathol 52: 89-99.

Zhu F, Gu C, Cheng G, Su J, She R, Hu X**(2007)** Dynamic distribution of new type duck hepatitis virus in experimental infectious duckling. Huazhong Agric Univ 26: 511-513.

Zhu J, Zhang Y, Ghosh A, Cuevas RA, Forero A, Dhar J, Ibsen MS, Schmid-Burgk JL, Schmidt T, Ganapathiraju MK, Fujita T, R. Hartmann R, Barik S, Hornung V, Coyne CB, Sarkar SN**(2014)** Antiviral activity of human OASL protein is mediated by enhancing signaling of the RIG-I RNA sensor. Immunity 40: 936-948.

Zhu Y, Wang M, Cheng A, Zhu D, Jia R, Liu M, Chen S, Zhao X, Yang Q, Wu Y, Chen X **(2018)** Distribution of duck hepatitis A virus type 3 in artificial infected ducklings and analysis of the relationship between histopathological changes and expression of cytokines in the livers. Acta Vet Zootech Sin 49: 164-172.